

Interrupted SAR operation and classification performance

R. J. A. Tough, K. D. Ward, P. W. Shepherd
TW Research Ltd, Harcourt Barn,
Harcourt Road, Malvern, WR14 4DW

Abstract

A SAR system can be made compatible with other interleaved modes if the impact of the interruptions in operation necessary to accommodate these can be ameliorated. A technique, phase shift cancellation, which effectively eliminates many of the artefacts of interrupted operation is described and analysed. The performance of a template matching classifier is shown to be degraded significantly by interrupted SAR operation, and that, for modest rates of interruption, this performance can be recovered by PSC processing of the image prior to classification. It is shown that this approach is compatible with interrupted SAR processing of data taken from a fast-moving (circa Mach 1) platform.

Keywords: Multi-mode operation, interrupted SAR, phase shift cancellation, classification performance.

Introduction

Combat aircraft fire-control radars, such as APG-77 for F/A-22, APG-81 for F-35(JSF), APG-79 for F/A-18 and Captor for Typhoon, have multiple modes for search, track and identification of airborne targets. These modes are interleaved to carry out all the functions simultaneously, a feature that is necessary in such a dynamic environment. The radars also have (or are developing) surface SAR imaging modes. These SAR modes require the radar to suspend all other activities in order to acquire the continuous data required for SAR imagery. Even with active electronic scanning, the interruption time to allow typical pulsed-Doppler bursts for updating airborne targets is too long to be accommodated within standard SAR processing. The development of an interrupted SAR (InSAR) mode would allow these fire-control radars to continue to be truly multi-mode even when acquiring SAR data.

In an earlier paper [1] we discussed the implications of InSAR operation in some

detail, characterising the side-lobe artefacts that arise in terms of a point spread function. The close connection between SAR image formation and Fourier sampling and reconstruction was stressed, and provided the basis for our formal analysis. Attempts to enhance the InSAR image by recovering the Fourier components, omitted as a consequence of interrupted operation, by conventional interpolative techniques proved to be unsuccessful; their underlying numerical instability was recognised as being characteristic of many ill-posed inversion problems. An alternative method for side-lobe suppression, based on apodisation of the interrupted aperture, was suggested, and shown to be stable and effective in the presence of significant levels of noise. In this paper we discuss this phase shift cancellation (PSC) technique in a more depth than was done in [1], and assess its usefulness in the recovery of classification performance that is lost due to interrupted operation. The latter analysis is carried out using a template matching classifier, whose operation we discuss in

some detail. Finally we consider a ‘real world’ scenario in which InSAR operation would be advantageous, and show that this should be achievable using the techniques we have developed.

Phase shift cancellation processing

The connection between SAR imaging and Fourier analysis has been emphasised by Walker [2], and is exploited extensively in [1]. Range resolution is acquired from the frequency content of the transmitted signal; the relative motion of the platform and target provides the Fourier information that furnishes us with resolution in the azimuthal direction. Here we will focus our attention on the latter process. The selection of the Fourier components can be represented by a weighting $H(k)$ in k space; the image obtained is then described in terms of a point-spread function (PSF) given by

$$W(x) = \int \exp(ikx)H(k)dk. \quad (1)$$

The effects of interrupted operation are captured by the function $T(k)$, which takes the value zero during interruption, and unity elsewhere. The PSF appropriate to interrupted operation is

$$W_{\text{int}}(x) = \int \exp(ikx)H(k)T(k)dk \quad (2)$$

We now displace the interruptions $T(k)$ to the synthetic aperture slightly, but leave the overall weighting function $H(k)$ unchanged; in practice this is achieved by excising a small part from each sub aperture prior to SAR processing, either symmetrically or wholly from either end. When this is done the phases of the side-lobe contributions will shift, as a consequence of the Fourier shift theorem, while that of the main lobe is un-altered. Let us consider the regular interrupt function ($\alpha = \delta/\Delta$)

$$T(k) = 1, \quad |k - n\Delta| \leq \frac{\delta}{2}, \quad n = 0, \pm 1, \pm 2 \dots \quad (3)$$

$$= 0, \quad \text{otherwise}$$

for which

$$W_{\text{int}}(x) = \frac{1}{\pi} \sum_{m=-\infty}^{\infty} W(x - 2m\pi/\Delta) \frac{\sin(m\delta\pi/\Delta)}{m} \quad (4)$$

$$\approx \alpha W(x) + \frac{\sin(\pi\alpha)}{\pi} W(x - 2\pi/\Delta)$$

where, in the second step, we have retained only those terms making a contribution in the region of a principal side-lobe. The corresponding shifted interrupt PSFs can be written as

$$W(x)_{\text{ap}} = \frac{1}{\pi} \sum_{m=-\infty}^{\infty} W(x - 2m\pi/\Delta) \frac{\sin(m\pi\delta/\Delta)}{m} \exp(\mp 2i\eta m\pi/\Delta)$$

$$\approx \alpha W(x) + \frac{\sin \pi\alpha}{\pi} W(x - 2\pi/\Delta) \exp(-2i\eta\pi/\Delta) \quad (5)$$

Thus, if we form the three images from the shifted interrupted data we associate three complex numbers with each point x , which we can represent as

$$z_1 = a + b$$

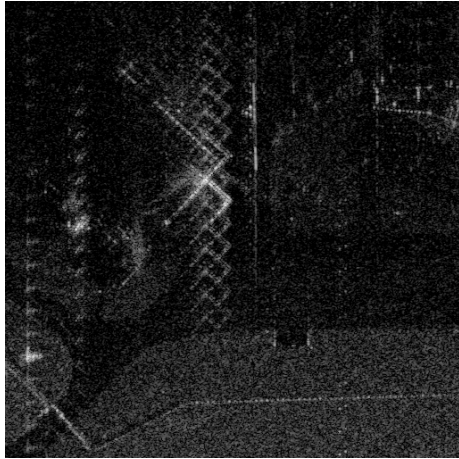
$$z_2 = a + b \exp(i\phi) \quad (6)$$

$$z_3 = a + b \exp(-i\phi)$$

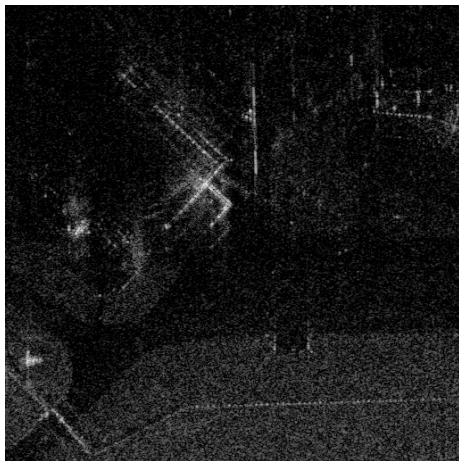
Given the measured fields z_1, z_2, z_3 we can now eliminate b, ϕ from (6) to determine the main lobe field, a , as

$$a = \frac{z_2 z_3 - z_1^2}{z_2 + z_3 - 2z_1}. \quad (7)$$

A processing scheme that implements this simple analysis has been applied to both simulated and real SAR data. Its effect is demonstrated in Figures 1a and 1b. The former shows a 10% interrupted SAR image with characteristic side-lobes; these are very much reduced when the PSC algorithm is applied, as can be seen in Figure 1b.



(a)



(b)

Figure 1: Interrupted SAR images of a complex scene before (a) and after (b) PSC

We see from the expansions (4), (5) that the phase variation simple model for the phase shifted PSF (6) provides an approximation that motivates the PSC processing (7). In the case where the overall weighting has the familiar Hanning form

$$H(k) = 1 + \cos\left(\frac{2\pi}{(2N+1)\Delta}\right), \quad |k| \leq (N+1/2)\Delta$$

$$= 0, \text{ otherwise}$$

(8)

it is possible to evaluate the phase shifted PSF explicitly and so check the validity of (6). Inspection of (5) reveals that the phase variation in the shifted PSFs is ‘carried’ by

the un-interrupted PSF $W(x)$; when this falls off rapidly phase variations are localised in the regions occupied by the side-lobes and (6) provides a reasonable representation of this behaviour. In the case of the Hanning weighting $W(x)$ is sufficiently localised for this to occur. The sinc form of $W(x)$ associated with a ‘top-hat’ weighting falls off so slowly that (6) breaks down; application of (7) to the interrupted PSF in this case obliterates it entirely. Detailed calculations based on the Hanning weighted aperture also provided some insight into ‘glitches’ observed in noise free simulations [1] in the vicinity of zeroes of the $\sin(\delta x/2)/x$ weighting characteristic of a single sub-aperture; in practice these are completely overwhelmed by the presence of noise. Having described the PSC method, and highlighted some of the reasons for and restrictions on its usefulness, we will now consider its application to the recovery of classification performance degraded by InSAR operation.

The performance of a template matching classifier

To achieve some quantitative assessment of this application of InSAR we must first standardise the classifier and the task it performs. The template matching classifier (TMC) is familiar and reasonably well understood; we choose this as our benchmark processing. The TMC will be required to classify the orientation of a tank target, embedded in a background provided by a real SAR image of a complex scene incorporating several large man-made objects. Performance can be quantified in terms of probabilities of correct and incorrect classification. This in turn is based on the ranking of values taken by the correlation function of the image and a set of known templates. This correlation function consists of target and background derived contributions. Introducing the Fourier transforms of the template, target

signal and background noise ($\tilde{t}(\mathbf{k}), \tilde{s}(\mathbf{k}), \tilde{n}(\mathbf{k})$ respectively) we can write these as

$$y_s(\mathbf{r}) = \frac{1}{(2\pi)^2} \int d^2 k \exp(-i\mathbf{k} \cdot \mathbf{r}) \tilde{t}(\mathbf{k}) \tilde{s}(\mathbf{k})^* \quad (9)$$

$$y_n(\mathbf{r}) = \frac{1}{(2\pi)^2} \int d^2 k \exp(-i\mathbf{k} \cdot \mathbf{r}) \tilde{t}(\mathbf{k}) \tilde{n}(\mathbf{k})^*$$

A measure of the effectiveness of the template in bringing out the target signal from the background is provided by ‘signal to noise ratio’ of the output of the correlator at point \mathbf{r} :

$$\text{SNR} = \frac{1}{(2\pi)^4} \frac{\left| \int d^2 k \tilde{t}(\mathbf{k}) \tilde{s}(\mathbf{k})^* \exp(-i\mathbf{k} \cdot \mathbf{r}) \right|^2}{\int d^2 k \left| \tilde{t}(\mathbf{k}) \right|^2 W_n(\mathbf{k})}. \quad (10)$$

Here $W_n(\mathbf{k})$ is the power spectrum of the background noise process. A template that maximises this signal to noise ratio for a given signal $s(\mathbf{r})$ can now be identified as

$$\tilde{t}(\mathbf{k}) = \alpha \frac{\tilde{s}(\mathbf{k})}{W_n(\mathbf{k})} \exp(i\mathbf{k} \cdot \mathbf{r}) \quad (11)$$

When the background noise process is uncorrelated (‘white’) and has a constant power spectrum, we would see the best SNR value when the template and target structure coincide. Here we see how the take account of the correlation structure of the background through the introduction of its power spectrum into the denominator of the template’s frequency space representation; this both ‘whitens’ the background component of the correlator output, and takes account of the resulting distortion of the target structure signature. The maximisation of SNR is an *ad hoc* identifier for good classifier performance when the background noise has arbitrary single point statistics. In the case where the background noise is Gaussian, however, it leads us to the processing scheme that is optimal. These insights have been incorporated into our classification processing, through the ‘de-trending’ of the imagery in an attempt to impose stationary and approximately Gaussian statistics on the background, and the incorporation of

the power spectrum of this background into the matched template.

When detecting a target signal in this way we will not, in general, know its position *a priori*. Consequently the global maximum of the correlator output must be identified and thresholded to ascertain whether the target is present; the location of the global maximum can then be assigned to that of the target feature. A realistic analysis of the performance of this correlation processing must thus be based on the statistics of the global maximum of a sample (of known size) of the Gaussian random field modelling the correlator output. A simple heuristic route to the properties of the global maximum of a correlated Gaussian process is provided by the order statistics concept [3]. This process will exhibit local maxima, taking values x . As a consequence of the de-correlation of the underlying process, these local maxima will be effectively independent; a well-defined number N of these maxima will be found within a sample of the Gaussian process of a given size. Thus we have, in effect, N samples of an independent random variable x , to which we assign a, as yet unspecified, PDF $P(x)$. The probability that all of these locally maximum values are less than or equal to X (i.e. X is the global maximum) is given by

$$\text{Prob}\{\forall x \leq X\} = \left(\int_{-\infty}^X P(x) dx \right)^N \quad (12)$$

The probability that the global maximum exceeds X is therefore given by

$$1 - \left(\int_{-\infty}^X P(x) dx \right)^N; \quad (13)$$

this simple result enables us to evaluate probabilities of false alarm and detection.

To implement this simple approach we must be able to relate the constituents of our model, the pdf of the locally maximum values and the number of local maxima in a

sample of the process of a given size, to the properties of the underlying correlated Gaussian process. In the case of a two-dimensional random field, this analysis has not yet been completely developed. Its underlying principles were established by Longuet-Higgins [4] and have been re-considered more recently by Hill, Tough and Ward [5]. While the PDF has not been determined for the full range of locally maximum values, the form taken by the ‘tail’ is known and determines the probability that the global maximum of a random field of reasonable size exceeds a threshold. This work has been extended to incorporate the contributions of both $y_n(\mathbf{r})$ and $y_s(\mathbf{r})$ into the model; probabilities of detection and false alarm can now be evaluated straightforwardly. Figures 2 and 3 compare calculated and simulated results for the variation of probability of detection with the threshold set for the global maximum and the ROC plot of probability of detection vs. that of false alarm. In each case the agreement is satisfactory.

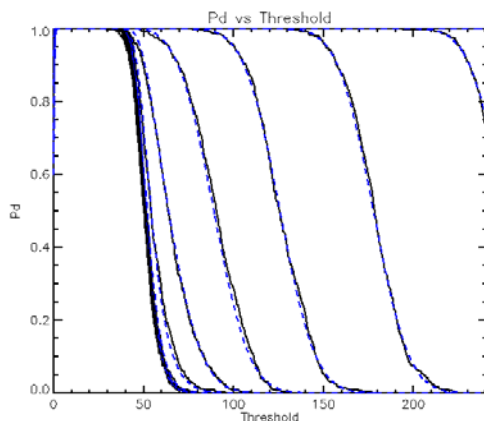


Figure 2: Variation of probability of detection with threshold; SNR incremented by 3dB, from 12 dB.

The impact of InSAR on classification performance

Simulations have been carried out to assess the impact of interrupted operation on the performance of the TMC against orientations of a tank target in uniform and

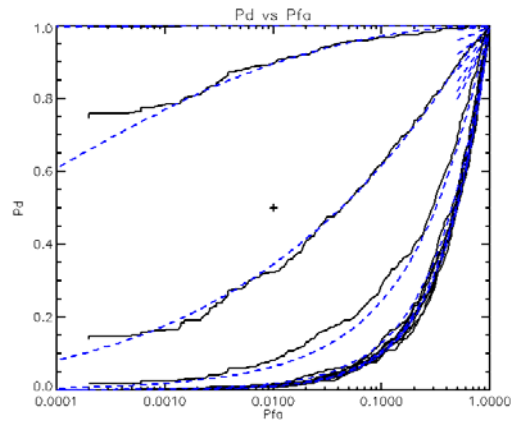


Figure 3: ROC curves: SNR incremented by 3db, from 12 dB.

complex backgrounds. Interrupted operation is found to degrade classification performance quite significantly: an increase in SNR of between 5 and 15 dB is required to re-establish a greater than 50% rate of correct classification. In the idealised, uniform background, case it is a relatively simple matter to recover much of this lost performance, simply by introducing templates that incorporate the delocalised side-lobe structure characteristic of interrupted operation. This technique is effective, even for significant (>50%) levels of interruption. When it is applied to the target in a complex environment, however, this is no longer the case, especially for higher interruption rates. This observation can be understood in terms of the delocalised interrupted template interacting with features in the background; the residual degradation in classification performance is greater when the target is close to such features. PSC effectively localises the InSAR target signature by eliminating its side-lobes; once this has been done classification by matching to the un-interrupted template can be carried out. We have found that this approach works satisfactorily for relatively small ($\leq 15\%$) rates of interruption. As we shall see in the next section, InSAR operation in this regime is potentially very useful.

An operational example

Typically, the time-critical functions (such as the updating of tracks on threat targets) impose an upper limit on the resolution achievable from a SAR in continuous operation. With InSAR, this limit is relaxed. Thus, for example, a five-fold increase in resolution can be obtained for a practically feasible interruption rate of 10%. The resolution cell size ρ for a SAR system is given by

$$\rho = \frac{\alpha\lambda R}{2vT \sin(\theta)}; \quad (14)$$

α accounts for the windowing needed to control sidelobes (typically 1.4), λ is the radar wavelength, R is the range to the image scene, v is the radar platform velocity, T is the coherent SAR aperture time, and θ is the angle between the radar platform track and the direction of the image scene from the radar.

At X Band ($\lambda = 0.03$ m) for a fast jet moving at speed $v=300$ ms⁻¹ and imaging at a bearing of 30° and a range of 100 km, a requirement to update threat target tracks every 10 seconds (total update time, say, 1 second) would limit the uninterrupted SAR resolution to about 1.5 m. This is not sufficient for meaningful ATRI. A modest interruption ratio of 10%, and an increase of the overall aperture time to 50 seconds, would produce a resolution of 30 cm, which would allow ATRI to be performed.

Conclusions

This paper has outlined some concepts that might facilitate the interrupted operation of a SAR system, to allow time critical functions to be performed and at the same time provide a resolution capability consistent with the requirements of target classification in complex environments. A novel and robust method (PSC) for the suppression of the side-lobes typical of InSAR has been developed and is now well understood. The performance of a template matching classifier, applied to a tank target in a complex environment, has been

modelled in some detail, and provided a benchmark for the assessment of the impact of InSAR operation on classification performance and the extent to which it can be ameliorated. We have shown that PSC can recover satisfactory performance for a system with circa 10%-15% interrupted operation, and that such a capability can be operationally significant. While we have demonstrated that this strategy could work in principle, much remains to be done, to optimise its implementation and performance, and so help ensure that it would work in practice.

References

1. R.J.A. Tough, K.D. Ward and P.W. Shepherd, 'The enhancement of interrupted SAR imagery', A26, 3rd EMRS DTC Technical Conference, 2006
2. J.L. Walker, 'Range-Doppler imaging of rotating objects', IEEE Trans. Aerospace and Electronic Systems, **AES-16**, 23-52, 1980
3. B.W. Lindgren, 'Statistical theory', 3rd edn., Section 4.3.2, Macmillan, New York, 1976
4. M.S. Longuet-Higgins, 'Statistical analysis of a random moving surface.', Phil. Trans. Roy. Soc., **A249**, 321-388, 1957
5. R.D. Hill, R.J.A. Tough and K.D. Ward, 'The distribution of the global maximum of a Gaussian random field and the performance of matched filter detectors', IEE Proc. Vis. Image Signal Process., **147**, 297-903, 2000

Acknowledgements

The work reported in this paper was funded by the Electro-Magnetic Remote Sensing (EMRS) Defence Technology Centre, established by the UK Ministry of Defence and run by a consortium of Selex, Thales Defence, Roke Manor Research and Filtronic.